

VHDL-AMS based modeling and simulation of mixed-technology microsystems: a tutorial[☆]

Pavel V. Nikitin*, C.-J. Richard Shi

Mixed-Signal CAD Research Laboratory, Department of Electrical Engineering, University of Washington, Seattle, WA 98195, USA

Received 23 March 2005; received in revised form 2 December 2005; accepted 5 December 2005

Abstract

This tutorial paper describes different approaches to modeling and simulation of mixed-technology microsystems that consist of electrical circuits connected to subsystems described by partial differential equations (PDEs), which is a typical situation in many modern integrated circuits and systems.

We target this paper towards the audience use of VHDL-AMS (a hardware description language suitable for modeling and simulation of such systems). We describe existing approaches to modeling such systems and present three examples accompanied by their VHDL-AMS implementations and simulation results.

© 2006 Elsevier B.V. All rights reserved.

Keywords: VHDL-AMS; Modeling; Simulation; Mixed-technology

1. Introduction

What are mixed-technology microsystems? These are miniature integrated systems composed of parts (subsystems), such as digital electronic blocks or various sensors, which belong to different physical domains (electrical, electromagnetic (EM), thermal, mechanical, etc.). Examples include micro-electro-mechanical systems (MEMS) [1,2], systems-on-chip (SoC), systems-on-package (SoP), etc. [3]. These systems become ubiquitous and find many applications in engineering, medicine, biology, and other areas [4,5]. Modeling and simulation of such systems is a challenging task due to the presence of multi-physics effects and their interaction.

An attractive and often the only feasible way to simulate such complex systems in a reasonable amount of time is to use behavioral models to simplify physics and explore interaction between different domains. A modeling environment naturally suited for behavioral modeling of mixed-technology problems is VHDL-AMS [6–8]. This high-level hardware description language is an IEEE standard and extension of a digital language VHDL [9]. VHDL-AMS is widely used in electronic design flow for modeling various mixed-signal (analog and digital) circuits and systems including such recent applications as RFID systems [10]. It can also be used to model mixed-technology systems if their description is limited to differential algebraic equations (DAEs) [11]. Due to the complexity, the support for partial differential equations (PDEs) was intentionally left out of VHDL-AMS [12]. This imposes a restriction on accurate modeling of subsystems with distributed physics effects. A proposition to extend the capability of VHDL-AMS to support PDEs has appeared in the literature [13] but is a challenging task and remains a work in progress.

There exist multiple publications on general behavioral modeling and simulation of microsystems [14–16]. For example, a recent publication [17] presents a good overview

[☆]This research was supported in part by US Defense Advanced Research Projects Agency NeoCAD program under Grant N66001-01-1-8920 and an NSF CAREER Award under Grant no. 9985507.

*Corresponding author. Now with Intermec Technologies Corporation, 6001 36th Ave W, Everett, WA 98203, USA. Tel.: +1 425 267 2939; fax: +1 425 355 9551.

E-mail addresses: pavel.nikitin@intermec.com (P.V. Nikitin), cjshi@ee.washington.edu (C.-J.R. Shi).

of using two modern high-level hardware description languages VHDL-AMS and Verilog-AMS for modeling mixed-technology systems when convenient physical behavioral models are already available for all subsystems.

In this paper, we focus on a general category of mixed-technology systems that consist of electrical circuitry connected to a subsystem described with PDEs for which no behavioral model is available a priori. We show how such systems can be modeled and simulated in time domain within the framework of VHDL-AMS. We describe two major approaches to modeling and simulation of such systems, discuss their advantages and drawbacks, and present three examples. We target this paper towards the use of VHDL-AMS and intentionally keep our examples simple for clear demonstration of all steps involved into modeling and simulation process. The methods we describe are not VHDL-AMS-specific and can be implemented in other behavioral modeling languages such as Verilog-AMS.

2. Mixed-technology microsystem

A system restricted to one physical domain can be modeled and simulated by numerically solving a set of specific equations that describe the physics of the system for a given set of geometry, sources, and boundary conditions. For example, electrical circuits can be described with Kirchhoff's equations. Other physics (mechanics, acoustics, electromagnetics, etc.) can often be described with PDEs.

There exist several excellent domain-specific simulators (e.g. *SPICE* [18] for electrical circuits, *Ansys Mechanical* [19] for mechanical systems or *Ansoft HFSS* [20] for EM problems) which are very convenient for solving physical problems restricted to one specific domain. Options, parameters, and boundary conditions can usually be specified from within a user interface of the simulator. However, a description of a complete mixed-technology system often cannot be restricted to one physical domain. Moreover, many subsystems usually need to be simulated concurrently (e.g. in time domain).

Some domain-specific simulators (*Ansys Multiphysics* [19], *Ansoft Designer* [20], *FEMLAB* [21], etc.) have capabilities to include circuits in their physics-based simulations. However, these capabilities are not yet at the level sufficient for modeling complex mixed-technology systems (especially if they include digital circuitry and nonlinear analog circuits) and do not have the flexibility offered by VHDL-AMS.

Coupling a domain-specific simulator and a circuit simulator is possible but the process of connecting two simulators is challenging and different in each particular case due to the lack of commonly accepted modeling environment and hence a necessity to know the details of inner workings of both circuit simulator and domain-specific simulator. The fact that several different time scales are present in multi-physics simulation presents an addi-

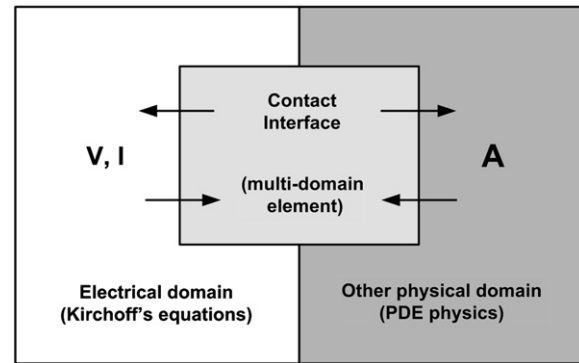


Fig. 1. Mixed-technology microsystem.

tional difficulty in coordinating the operation and interaction of circuit and domain-specific simulators [22].

As an example, consider a subsystem whose physics is described with PDEs and which is connected to some electrical circuit. To solve the PDE problem, one needs to know:

- PDEs describing the physics,
- parameters of the PDEs,
- boundary conditions,
- contact interface details.

Contact interface specifies how various physical quantities interact with circuit quantities. Exact definition of the contact interface depends on the physics of the problem and may involve a translation between physical quantities (e.g., how temperature and heat flow through the element relate to its voltage and current).

Assume that subsystem's physics can be described by a single second-order one-dimensional (1-D) PDE of the following form:

$$\frac{\partial^2 A}{\partial x^2} + \alpha(x, t) \frac{\partial A}{\partial t} = f(x, t), \quad (1)$$

where $A(x, t)$ is the quantity of interest, $\alpha(x, t)$ is the parameter, $f(x, t)$ is the excitation, x is a spatial variable, and t is time. To solve (1), we need to know $\alpha(x, t)$, which contains the information about material properties and geometry of the system, and the boundary conditions for $A(x, t)$, which also include the initial conditions. We also need to define how the quantity $A(x, t)$ interacts with circuit quantities. Usually, interaction between domains happens through a multi-domain element (a part of the system which simultaneously belongs to two or more different domains) as shown in Fig. 1.

3. Modeling and simulation

3.1. Modeling approaches

There exist two major approaches to time-domain modeling and simulation of mixed-technology circuit-

PDE systems. Both approaches can be implemented in VHDL-AMS and are described below.

The first approach is coupled modeling: combining all equations from all subsystems together and solving them simultaneously; to realize that within a framework of one language and one simulator, one has to convert PDEs to DAEs. This can be achieved by spatial discretization of PDEs which leaves the time derivatives intact to be handled by a time-domain solver, central to any VHDL-AMS or circuit simulator. Stand-alone spatial discretization has been used before for solving PDE problems via equivalent circuits in SPICE [23].

The second approach is macromodeling: using behavioral macromodel based on simulation results from specialized solvers. A macromodel can be an equivalent circuit that can be directly used in SPICE and other circuit simulators or a compact reduced-order model. The latter is essentially a set of reduced order ordinary differential equations which approximate the behavior of a complex subsystem. Compact models become increasingly popular as they can also be interfaced to circuits [24]. This approach becomes extremely important for speeding up simulations of complex multi-physics systems, such as coupled circuit-electromagnetic systems [25] and MEMS devices [26].

3.2. Simulators

The fact that both modeling approaches can be implemented in VHDL-AMS and thus fit into an electronic design flow is important from a practical point of view because it allows a designer to use standard modeling and simulation tools.

A number of various commercial VHDL-AMS simulators are currently available from several electronic design automation (EDA) companies. Those simulators include *Virtuoso AMS Designer* from Cadence [27], *ADVance MS* from Mentor Graphics [28], *SMASH* from Dolphin [29], *Simplorer* from Ansoft [20], etc. Some of these simulators provide libraries of functional blocks that fit into their design flows and allow one to perform simulations at different levels of abstraction from the same environment. This is especially valuable when analog circuits are added to previously designed digital blocks. In addition to the simulators mentioned above, there is also a number of model compilers capable of compiling a VHDL-AMS behavioral model of a device into circuit simulator code [30,31].

Different simulators provide different support for VHDL-AMS language; some constructs may be supported in one simulator and not supported in another. In this paper, all VHDL-AMS simulations have been done with simulator *SMASH* [29] which supports most of IEEE standard VHDL-AMS. The examples given below have been written accordingly and targeted to compile and run on this particular simulator. Porting them to another simulator may require some modifications depending on the VHDL-AMS language support of the simulator.

Below, we present three examples that illustrate the two modeling approaches described above.

4. Example 1: transmission line (1-D)

4.1. System description

Consider a system that consists of a 1-D transmission line connected to a circuit as shown in Fig. 2. The transmission line can represent e.g. an integrated circuit interconnect [32] or an acoustic MEMS delay line [33]. The signal propagation on this transmission line can be described with the wave equation (a second-order PDE), which we will implement in VHDL-AMS using coupled modeling approach (PDE discretization) shown in [34].

The system has four electrical nodes: $n1$, $n2$, $n3$, and ground. The interaction between the transmission line subsystem and the circuit takes place via terminal voltages and currents. In this example, the internal quantities of the PDE subsystem (voltages and currents) are the same as circuit variables, thus no translation is needed.

4.2. Physical model

If the transmission line is lossless, the wave equation has the form [35]

$$-\frac{\partial^2 V}{\partial z^2} - \beta^2 \frac{\partial^2 V}{\partial t^2} = 0, \quad (2)$$

where V is the voltage on the transmission line and $\beta = \sqrt{LC}$ is the propagation constant (L and C are the inductance and capacitance per unit length). The same problem can be equivalently formulated in terms of Telegrapher's equations:

$$-\frac{\partial V}{\partial z} = L \frac{\partial I}{\partial t}, \quad -\frac{\partial I}{\partial z} = C \frac{\partial V}{\partial t}. \quad (3)$$

To transfer this description into VHDL-AMS, PDEs given by Eq. (3) need to be discretized with respect to z (e.g. using a classical central difference formula). Number of discretization points N for the transmission line of a given length determines the spatial step dz . The voltage and the current need to be determined at each point. A set of two PDEs given by Eq. (3) can be converted into the following

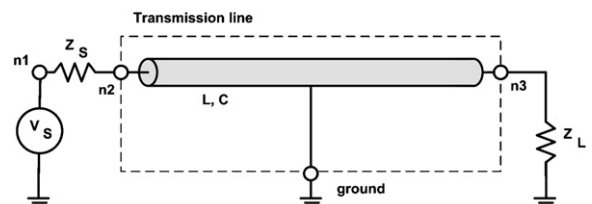


Fig. 2. Example 1: transmission line connected to an electrical circuit.

set of $2N$ ordinary differential equations (ODEs):

$$-\frac{V_n - V_{n-1}}{dz} = LI'_n, \quad -\frac{I_{n+1} - I_n}{dz} = CV'_n, \quad n = 1, \dots, N, \quad (4)$$

where V_n and I_n are currents and voltages at spatial points and prime ' denotes a derivative with respect to time. Two additional equations are given by Eq. (5) which defines boundary conditions for an interface to the circuit:

$$V_{in} = V_S - I_{in}Z_S, \quad V_{out} = I_{out}Z_L. \quad (5)$$

Note that in this discretization scheme voltages and currents are not defined at the same points in space which may cause matching errors and give rise to reflections even when all impedances are perfectly matched. This effect is known [36] and may require an introduction of correction elements to eliminate the errors. In general, the model described above is still accurate and valid if N is sufficiently large.

One can see that discretized equations for voltage and current on the transmission line are equivalent to circuit equations describing the N -section LC-ladder network shown in Fig. 3, where Ldz and Cdz are the inductance and the capacitance of each segment of the transmission line. The N -section ladder network is usually valid only for a certain frequency range. The number of sections in the network determines the accuracy of the wideband response of the transmission line needed when it is driven by digital circuits with sharp signal transitions.

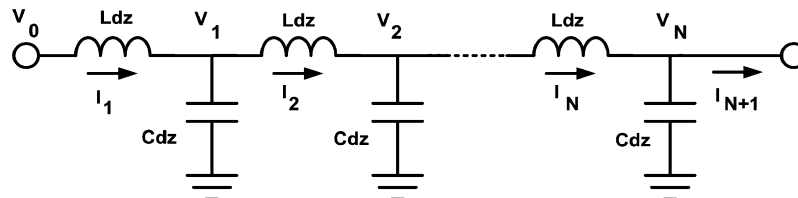


Fig. 3. Equivalent LC-ladder network for the transmission line in Example 1.

```

----- Testbench -----
LIBRARY IEEE; USE IEEE.electrical_systems.all, work.all;

ENTITY testbench_example_1 IS
  PORT(TERMINAL n1, n2, n3: ELECTRICAL);
END testbench_example_1;

ARCHITECTURE top OF testbench_example_1 IS
BEGIN
  VS: ENTITY pulse_source(simple)
    GENERIC map (amplitude => 1.0, delay =>10.0e-9, duration => 10.0e-9)
    PORT map (p => ELECTRICAL_REF, n => n1);
  RS: ENTITY resistor(simple)
    GENERIC map (resistance => 50.0)
    PORT map (p => n1, n => n2);
  TR: ENTITY transmission_line(behav)
    GENERIC map (Length => 0.5, L => 250.0e-9, C => 100.0e-12, N => 50)
    PORT map (a => n2, b => n3, g => ELECTRICAL_REF);
  RL: ENTITY resistor(simple)
    GENERIC map (resistance => 50.0)
    PORT map (p => n3, n => ELECTRICAL_REF);
END top;

```

Fig. 4. VHDL-AMS model for testbench in Example 1.

4.3. VHDL-AMS model

Figs. 4 and 5 present VHDL-AMS models for this example: for testbench architecture and for transmission line entity. The transmission line is 0.5m long with the distributed parameter values $L = 250.0$ nH/m and $C = 100$ pF/m. These are typical values for a microwave coaxial cable which result in characteristic impedance of 50Ω and signal propagation speed of $0.66c$. The source and the load resistors are $Z_S = 50\Omega$ and $Z_L = 50\Omega$. The transmission line has three terminals (input, output, and ground) and is discretized into N sections.

The contact interface is highlighted in the transmission line model. Since VHDL-AMS derivative attribute ('dot) is not supported in the GENERATE statement, vectors of time derivatives of voltage and current are created outside the loop. Note that I_{out} has a negative sign in front of it because of the VHDL-AMS definition of the current flowing into a terminal. For more information on reference directions of terminal quantities, see [8,37].

4.4. Simulation results

Fig. 6 shows the simulated transient source and load voltages in the transmission line example with rectangular pulse excitation for $N = 5$ and $N = 50$. These results match the analytical solution [38] given by Branin's model (which is also derived from Telegrapher's equations).

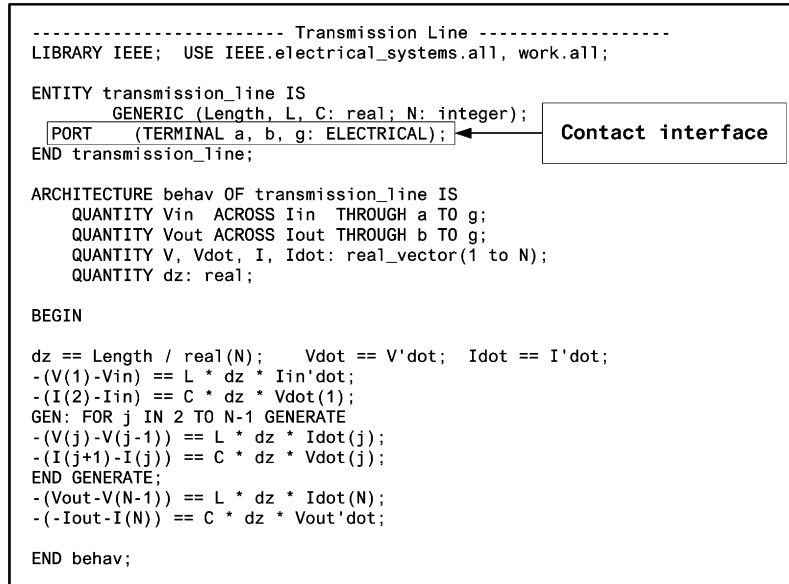


Fig. 5. VHDL-AMS model for transmission line entity in Example 1.

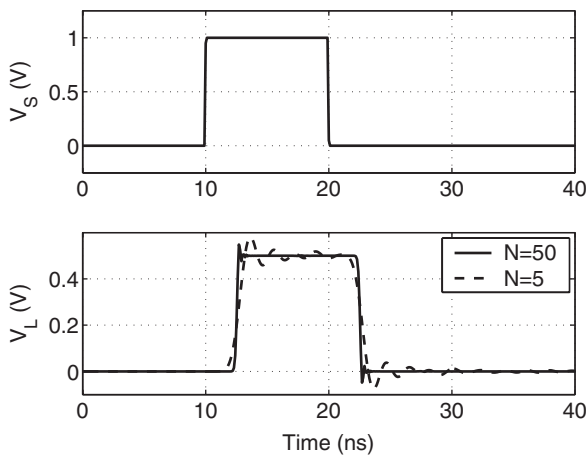


Fig. 6. Simulated source and load voltages for the transmission line in Example 1.

5. Example 2: electrothermal system (2-D)

5.1. System description

Consider now a system shown in Fig. 7 that consists of two electrical circuits coupled thermally via shared silicon substrate. Source V_1 and resistors R_1 and R_2 can represent a trigger line in the digital part of a mixed-signal system while source V_2 and resistors R_3 and R_4 can represent a biasing circuit in the analog part of the system.

Resistors R_2 and R_3 are electrothermal: they dissipate heat and their electrical performance is affected by their temperature. They are located on top of a rectangular silicon substrate of length L and width W . If the substrate material is uniform and $L \gg W$, this system can be considered to be two-dimensional (2-D). The temperature

distribution in the substrate can be described with the heat balance equation, which we will model in VHDL-AMS using coupled modeling approach shown in [39]. The approach is similar to the previous example but now deals with two dimensions.

The system has five electrical nodes: n_1 , n_2 , n_3 , n_4 , and ground. The interaction between the electrothermal subsystem and the circuit takes place via terminal voltages and currents. Electrothermal resistors R_2 and R_3 are multi-domain elements which act as contact interfaces between substrate thermal variables (temperature and heat flow) and circuit variables (voltage and current).

5.2. Physical modeling

Resistance of a typical electrothermal resistor can be written as [40]

$$R = R_0[1 + \alpha(T_r - T_0)], \quad (6)$$

where R_0 is the nominal resistance (at $T_0 = 300$ K), T_r is the resistor temperature, and α is the temperature coefficient of resistance. Both resistors R_2 and R_3 dissipate power and generate heat flux into the substrate, which affects their currents and temperatures. The substrate temperature T is given by the heat-balance equation

$$\frac{\partial T}{\partial t} = \frac{k}{\rho C} \left(\frac{\partial^2 T}{\partial x^2} + \frac{\partial^2 T}{\partial y^2} \right), \quad (7)$$

where x and y are the transversal coordinates, ρ is the material density, C is the specific heat capacity, and k is the thermal conductivity of the substrate. To spatially discretize Eq. (7) with respect to x and y , a finite difference discretization method can be used, similar to the previous example. We will assume that the thermal conductivity of these resistors is much larger than the conductivity of the

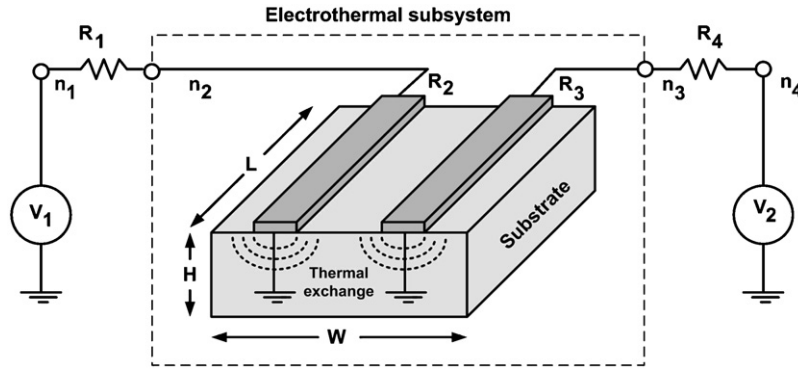


Fig. 7. Example 2: electrothermal subsystem connected to an electrical circuit.

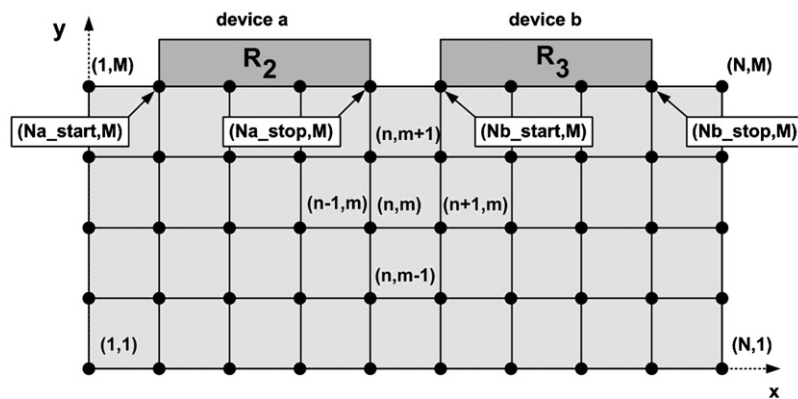


Fig. 8. Rectangular finite difference mesh for the substrate in Example 2.

substrate ($k_R \gg k$) so that temperature distribution inside resistors does not need to be modeled.

Consider a rectangular $N \times M$ mesh shown in Fig. 8 whose nodes are the points where the temperature needs to be determined spaced at $dx = W/(N - 1)$ and $dy = H/(M - 1)$. Electrothermal devices *a* and *b* (resistors R_2 and R_3) sit on top of several grid points. Resistor R_2 (device *a*) occupies points $(Na_start, M) - (Na_stop, M)$ and resistor R_3 (device *b*) occupies points $(Nb_start, M) - (Nb_stop, M)$.

Using the mesh given in Fig. 8, Eq. (7) can be discretized and rewritten as

$$\frac{\partial T}{\partial t} = \frac{k}{\rho C} \left[\frac{T_{n+1,m} - 2T_{n,m} + T_{n-1,m}}{(dx)^2} + \frac{T_{n,m+1} - 2T_{n,m} + T_{n,m-1}}{(dy)^2} \right]. \tag{8}$$

On the boundaries, terms in Eq. (8) which correspond to horizontal and vertical temperature gradients are replaced with $\pm P/kA$ on conductive boundaries (the surfaces of physical contact between the substrate and the resistors) and with $\pm h(T_a - T_{n,m})/k$ on convective boundaries (all other surfaces). Above, P is the power dissipated in a resistor, A is the area occupied by a resistor, and T_a is the

ambient temperature. The sign is determined by the boundary location.

Such discretization results in the system of $N \times M$ ODEs that can be solved in VHDL-AMS concurrently with the circuit equations. The temperature of each electrothermal resistor is computed by averaging the temperature over all grid points that lie immediately under the resistor surface:

$$T_{R_2} = \frac{\sum_{i=Na_start}^{Na_stop} T_{i,M}}{Na_stop - Na_start + 1}, \quad T_{R_3} = \frac{\sum_{i=Nb_start}^{Nb_stop} T_{i,M}}{Nb_stop - Nb_start + 1}. \tag{9}$$

5.3. VHDL-AMS model

Figs. 9 and 10 present VHDL-AMS codes for this example: testbench architecture and electrothermal subsystem entity. The electrothermal subsystem has four electrical terminals (two for each resistor) and includes a substrate and electrothermal resistors R_2 (device with terminals a1 and a2) and R_3 (device with terminals b1 and b2). The substrate is discretized into $N \times M$ points. We have used mathematical matrix package to define temperature as a 2-D array and a summing function to calculate the average temperature over several grid points.

```

----- Testbench -----
LIBRARY IEEE; USE IEEE.electrical_systems.all, work.all;

ENTITY testbench_example_2 IS
  PORT(TERMINAL n1, n2, n3, n4: ELECTRICAL);
END testbench_example_2;

ARCHITECTURE top OF testbench_example_2 IS
BEGIN
  V1: ENTITY pulse_source(simple)
    GENERIC MAP (amplitude => 10.0, delay =>25.0e-6, duration => 50.0e-6)
    PORT MAP (p => ELECTRICAL_REF, n => n1);
  R1: ENTITY resistor(simple)
    GENERIC MAP (resistance => 10.0)
    PORT MAP (p => n1, n => n2);
  EL: ENTITY electrothermal_subsystem(behav)
    GENERIC MAP (Width => 45.0, Height => 20.0, Length => 150.0,
      Ta => 300.0, T0 => 300.0, Ra => 10.0, Rb => 10.0,
      alpha=>0.1, N => 10, M => 5, Na_start => 2,
      Na_stop => 5, Nb_start => 6, Nb_stop => 9)
    PORT MAP (a1 => n2, a2 => ELECTRICAL_REF,
      a3=>n3, a4 => ELECTRICAL_REF);
  R4: ENTITY resistor(simple)
    GENERIC MAP (resistance => 10.0)
    PORT MAP (p => n3, n => n4);
  V2: ENTITY dc_source(simple)
    GENERIC MAP (amplitude => 2.0)
    PORT MAP (p => ELECTRICAL_REF, n => n4);
END top;

```

Fig. 9. VHDL-AMS code for testbench in Example 2.

For illustrative purposes, in this example we use the following mesh parameters: $N = 10$, $M = 5$, $Na_start = 2$, $Na_stop = 5$, $Nb_start = 6$, $Nb_stop = 9$. The values of circuit elements and geometrical dimensions of the problem were chosen so that the thermal coupling effect can be clearly seen. Those parameters were: $R_1 = R_2 = R_3 = R_4 = 10\ \Omega$ (at 300 K), $\alpha = 0.1\ \text{K}^{-1}$, $W = 45\ \text{mil}$,¹ $H = 20\ \text{mil}$, and $L = 150\ \text{mil}$. The properties of the silicon substrate and its boundaries were: $k = 1.412\ (\text{W/K cm})$, $\rho = 2.33\ (\text{g/cm}^3)$, $C = 0.7\ (\text{J/g K})$, $h = 1000\ (\text{W/cm}^2\ \text{K})$.

5.4. Simulation results

Fig. 11 shows transient voltages V_{R_2} and V_{R_3} on electrothermal resistors R_2 and R_3 . A constant 2 V DC source V_2 is turned on at $t = 0\ \mu\text{s}$. In the absence of the pulse from V_1 , this causes the voltage on R_3 to rise slowly due to self-heating until it reaches an equilibrium just above 1 V.

Source V_1 produces a $50\ \mu\text{s}$ long 10 V rectangular excitation pulse at $t = 25\ \mu\text{s}$. This causes initially a voltage of 5 V to appear across R_2 . The current heats up R_2 and generated heat propagates through the substrate to R_3 , increasing its temperature and voltage. In both cases (with and without the excitation pulse) voltage V_{R_3} stays the same until a certain time ($\approx 10\ \mu\text{s}$ from the beginning of the pulse) when the heat wave from R_2 reaches R_3 .

Fig. 12 shows calculated temperature distribution in the silicon substrate in the vicinity of resistor R_3 at the time moment $t = 200\ \mu\text{s}$. This distribution was obtained by calculating the temperature at each node using the VHDL-AMS model given in Fig. 10 (where $N = 10$ and $M = 5$)

and drawing isolines of constant temperature. Because of the large amount of heat dissipated in R_2 during the pulse, even after V_1 is turned off resistor R_2 continues to be a “warm spot” which primarily defines the temperature distribution inside the substrate.

6. Example 3: MEMS filter (3-D)

6.1. Description

Various structures that exhibit EM behavior (transmission lines, inductors, filters, etc.) play an important role in many modern VLSI SoCs and seriously affect their performance, especially at gigahertz frequencies. An example is MEMS structures which have been used for actuators, micromotors, and other applications [41,37,42–45]. High-frequency applications of MEMS structures include RF switches [46] and filters [47,48].

Consider the following system: MEMS comb finger structure driven by an external source as shown in Fig. 13. Three-dimensional (3-D) MEMS structure is a subsystem used here as an RF filter for which we will create a linear model to use in VHDL-AMS. The voltage source and the resistor represent a lumped circuit subsystem (which can be any transistor circuit). The system has four electrical nodes: $n1$, $n2$, $n3$, and ground. The interaction between the MEMS filter and the circuit takes place via terminal voltages and currents.

Because the 3-D geometry of the MEMS filter is rather complex, after meshing and discretization of PDEs (Maxwell’s equations which describe the EM behavior of this structure) it would result in a very high-order system of DAE equations. We will model this problem using macromodeling approach shown in [49].

¹1 mil = 0.0254 mm.

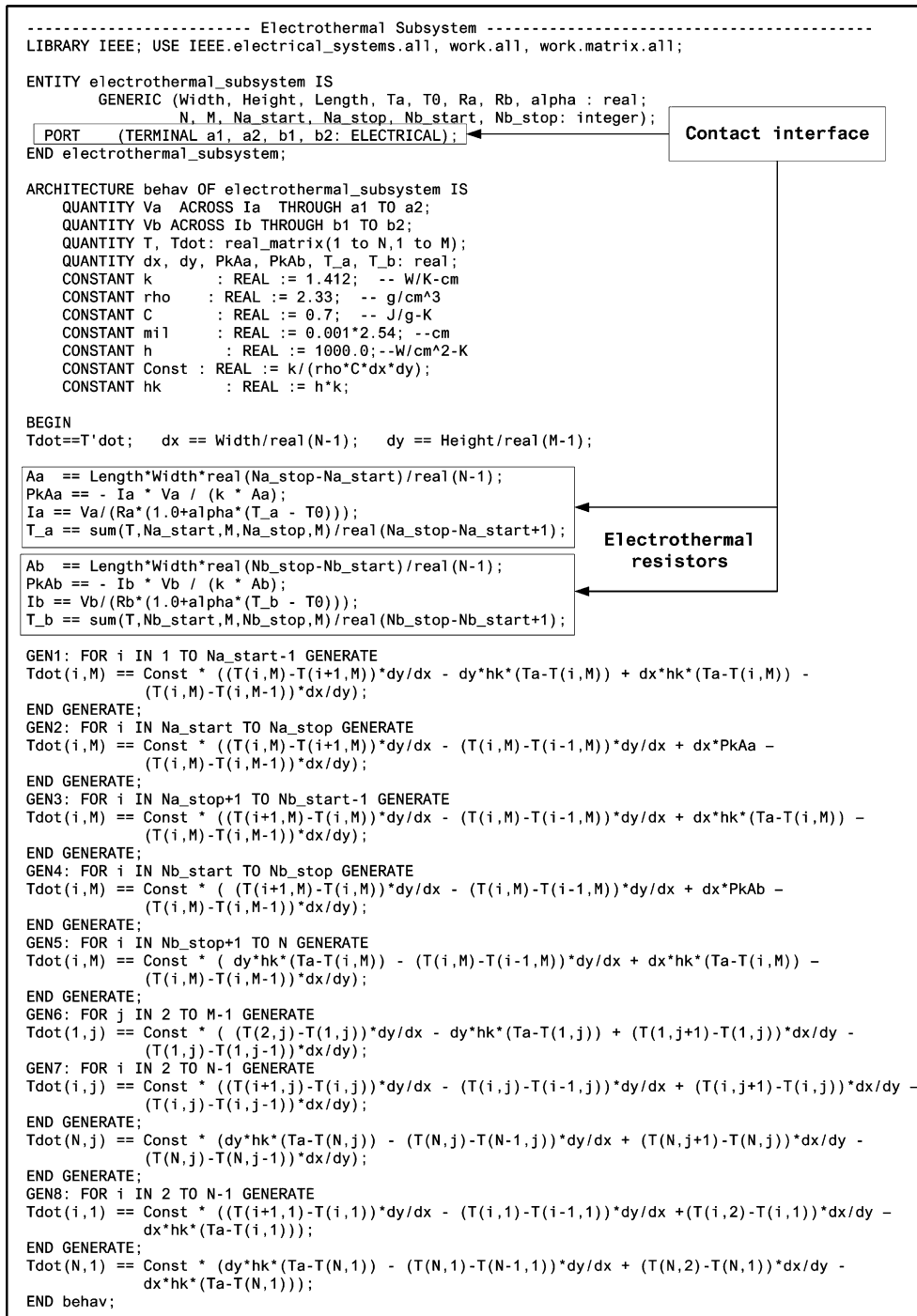


Fig. 10. VHDL-AMS code for electrothermal subsystem in Example 2.

6.2. Physical modeling

Typically, EM structures are measured or simulated in frequency domain using various EM simulators. There exist a great variety of numerical EM field solvers that allow modeling of on- and off-chip structures. To use S -parameters (or other frequency domain parameters) obtained from EM simulations in VHDL-AMS, frequency response can be approximated with the rational function to

obtain a time-domain macromodel suitable for subsequent use in VHDL-AMS simulator.

Knowing the frequency response allows one to identify a continuous transfer function $H(s) = b(s)/a(s)$ that approximates it where $a(s)$ and $b(s)$ are polynomials of a finite order that results in approximating the simulated frequency response. The desired order of the polynomials can be determined from the data. A number of different algorithms for extracting compact reduced

order models from frequency- or time-domain data are available [50,51].

In our example, a voltage source drives the MEMS filter connected to the load. The structure is 1 mm × 18 mm × 22 mm in size and positioned 1 mm above the ground plane as shown in Fig. 13. These dimensions were chosen for illustrative purposes to have a filter with the wide bandpass

response centered around 2 GHz. Smaller dimensions would result in higher operating frequency.

The filter was simulated in frequency domain using a finite-element software *Ansoft HFSS*. *S*-parameters obtained after simulation and approximated with the transfer

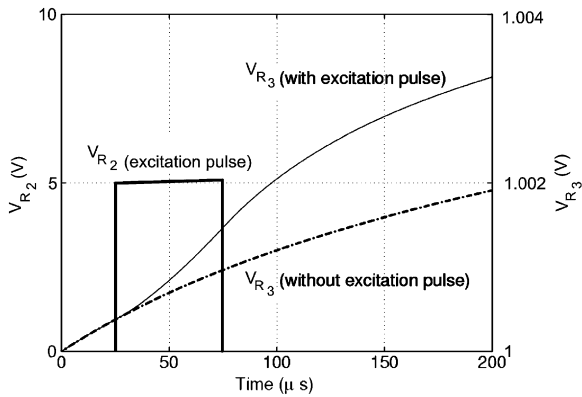


Fig. 11. Transient voltages V_{R_2} and V_{R_3} on resistors R_2 and R_3 in Example 2.

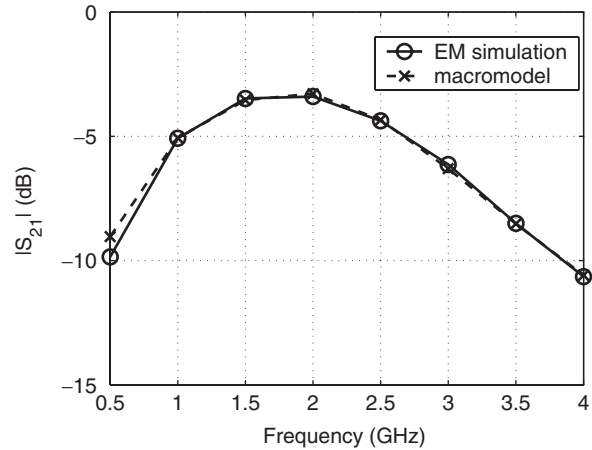


Fig. 14. Frequency response (S_{21} -parameter) of the MEMS filter in Example 3 shown in Fig. 13: simulated and approximated.

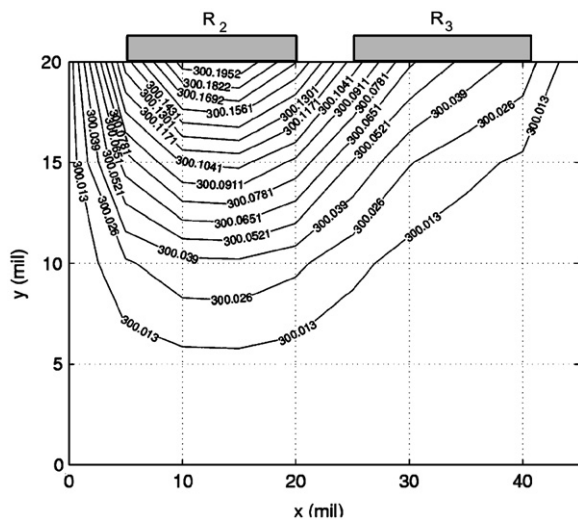


Fig. 12. Temperature distribution (kelvin) in the substrate in Example 2 at $t = 200 \mu s$.

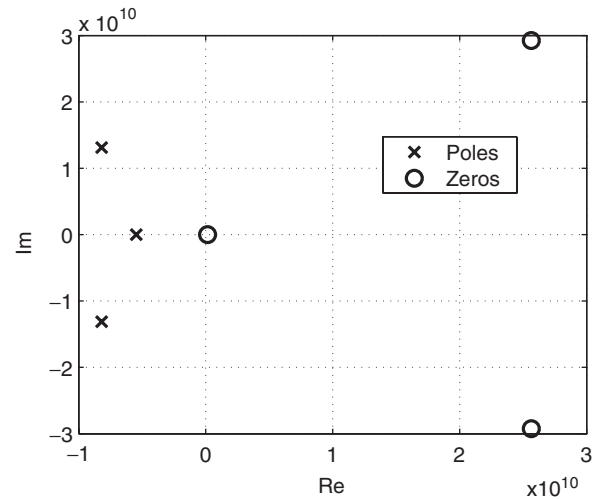


Fig. 15. Poles and zeros of the transfer function which approximates the frequency response in Fig. 14 for Example 3.

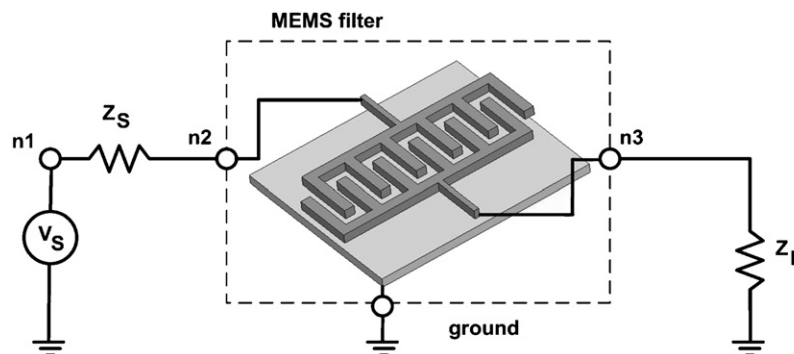


Fig. 13. Example 3: MEMS filter connected to a circuit.

function are shown in Fig. 14. For system identification in this example, we used *Matlab* function *invfreqs*. The third order transfer function whose poles and zeros are shown in Fig. 15 was sufficient to well approximate the wideband frequency response of the filter.

From the transfer function $H(s)$, one can easily construct a continuous time-domain macromodel in its classical

state-space form (see e.g. *Matlab* function *tf2ss*):

$$\begin{cases} \dot{\vec{x}} = \hat{A}\vec{x} + \hat{B}\vec{u}, \\ \vec{y} = \hat{C}\vec{x} + \hat{D}\vec{u}, \end{cases} \quad (10)$$

where $\vec{x}(t)$ is the vector of state variables, $\vec{u}(t)$ is the excitation and $\vec{y}(t)$ is the output signal. This state-space

```

----- Testbench -----
LIBRARY IEEE;
USE IEEE.electrical_systems.all, work.all, work.matrix.all;

ENTITY testbench_example_3 IS
    PORT(TERMINAL n1, n2, n3: ELECTRICAL);
END testbench_example_3;

ARCHITECTURE top OF testbench_example_3 IS

BEGIN

    VS: ENTITY gaussian_source(simple)
        GENERIC map (amplitude => 1.0, tau =>3.0e-9, T => 0.25e-9)
        PORT map (p => ELECTRICAL_REF, n => n1);
    RS: ENTITY resistor(simple)
        GENERIC map (resistance => 50.0)
        PORT map (p => n1, n => n2);
    MEMS: ENTITY mems_filter(behav)
        PORT map (a => n2, b => n3, g => ELECTRICAL_REF);
    RL: ENTITY resistor(simple)
        GENERIC map (resistance => 50.0)
        PORT map (p => n3, n => ELECTRICAL_REF);

END top;

```

Fig. 16. VHDL-AMS code for testbench in Example 3.

```

----- MEMS filter -----
LIBRARY IEEE;
USE IEEE.electrical_systems.all, work.all, work.matrix.all;

ENTITY mems_filter IS
    PORT (TERMINAL a, b, g: ELECTRICAL);
END mems_filter;

ARCHITECTURE behav OF mems_filter IS
    QUANTITY Vin ACROSS Iin THROUGH a TO g;
    QUANTITY Vout ACROSS Iout THROUGH b TO g;
    QUANTITY u, y, x1, x2, x3: real;

    CONSTANT Zo: real := 50.0;
    CONSTANT A11 : real := -2.1837e10;
    CONSTANT A12 : real := -3.2873e20;
    CONSTANT A13 : real := -1.3073e30;
    CONSTANT A21 : real := 1.0;
    CONSTANT A22 : real := 0.0;
    CONSTANT A23 : real := 0.0;
    CONSTANT A31 : real := 0.0;
    CONSTANT A32 : real := 1.0;
    CONSTANT A33 : real := 0.0;
    CONSTANT B1 : real := 1.0;
    CONSTANT B2 : real := 0.0;
    CONSTANT B3 : real := 0.0;
    CONSTANT C1 : real := -8.0705e9;
    CONSTANT C2 : real := 1.3129e20;
    CONSTANT C3 : real := -1.6934e29;
    CONSTANT D : real := 0.1102;

BEGIN

    u == Vin; y==Vout;
    x1'dot == A11*x1+A12*x2+A13*x3 +B1*u;
    x2'dot == A21*x1+A22*x2+A23*x3 +B2*u;
    x3'dot == A31*x1+A32*x2+A33*x3 +B3*u;
    y == C1*x1+C2*x2+C3*x3+D*u;
    Iout == Vout/Zo;

END behav;

```

Fig. 17. VHDL-AMS code for MEMS filter in Example 3.

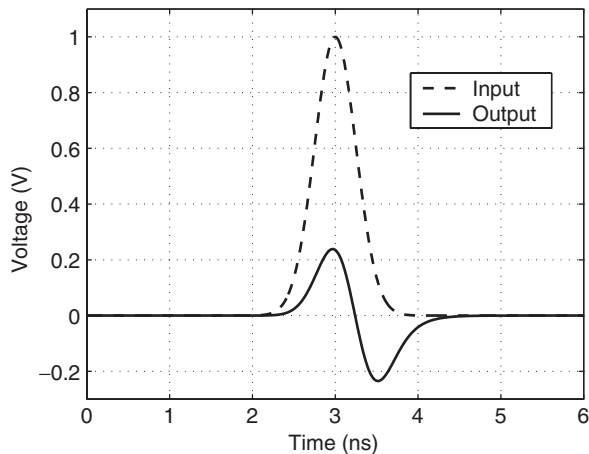


Fig. 18. Simulation results (input source voltage and output load voltage) for the MEMS filter in Example 3.

model contains an information about system dynamics sufficient for calculating system response to a general time domain excitation signal. The model is purely linear.

6.3. VHDL-AMS model

Figs. 16 and 17 present VHDL-AMS models for this example: testbench architecture and MEMS filter entity. The macromodel of the MEMS filter uses the excitation voltage from the source as the input $u(t)$ and the load voltage as the output $y(t)$. Note that some of the elements of matrices \hat{A} and \hat{B} are zeros.

Both source and load resistors are $50\ \Omega$. An excitation commonly used in EM and wireless communications problems is Gaussian pulse:

$$u(t) = u_0 e^{-(t-\tau)^2/2T^2}. \quad (11)$$

In our example, voltage source V_S generates a Gaussian pulse of the form with $u_0 = 1\ \text{V}$, $\tau = 3\ \text{ns}$, and $T = 0.25\ \text{ns}$.

6.4. Simulation results

Fig. 18 shows simulated transient input and output voltages for the MEMS filter for the Gaussian pulse excitation.

This example demonstrates that compact models (macromodels) are an accurate and efficient way of simulating coupled circuit-PDE problems in time-domain with VHDL-AMS. Compact models contain fewer internal variables than full EM problems and thus provide a significant simulation speedup.

In our example, the finite element mesh contained about 7500 tetrahedra and the wideband EM simulation took approximately 2 min of runtime on a 2 GHz PC. The VHDL-AMS simulation with third order macromodel

took about 1 s on the same PC resulting in about 100-fold gain in CPU time.

7. Conclusions

In this tutorial paper, we presented a VHDL-AMS based overview of different approaches to modeling and simulation of mixed-technology microsystems which consist of electrical circuits connected to subsystems described by partial differential equations (PDEs).

Modeling approaches can be classified into two major groups: coupled modeling and macromodeling, for which we presented three examples and their corresponding VHDL-AMS implementations. We intentionally kept our examples straightforward to demonstrate clearly all steps involved into the modeling and simulation process. These examples demonstrate that VHDL-AMS is well suited for modeling and simulation of complex mixed-technology systems.

The approaches described in this paper can be readily used in today's electronic design flow for including distributed physics effects into modeling and simulation process with VHDL-AMS or other high-level hardware description languages.

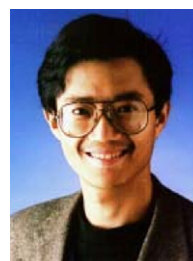
References

- [1] S.D. Senturia, CAD challenges for microsensors, microactuators, and microsystems, Proc. IEEE 86 (8) (1998) 1611–1626.
- [2] S.D. Senturia, Microsystem Design, 2001.
- [3] T.E. Zipperian, The second revolution—mixed-technology integrated microsystems, Device Research Conference, 2002, pp. 119–131.
- [4] K.D. Wise, D.J. Anderson, J.F. Hetke, D.R. Kipke, K. Najafi, Wireless implantable microsystems: high-density electronic interfaces to the nervous system, Proc. IEEE 92 (1) (2004) 76–97.
- [5] D. Uttamchandani, MEMS and microsystems engineering, IEE Proc. Sci. Meas. Technol. 151 (2) (2004) 53.
- [6] E. Christen, K. Bakalar, VHDL-AMS—a hardware description language for analog and mixed-signal applications, IEEE Trans. Circuits Syst. II Analog Digital Signal Process. 46 (10) (1999) 1263–1272.
- [7] A. Doboli, R. Vemuri, Behavioral modeling for high-level synthesis of analog and mixed-signal systems from VHDL-AMS, IEEE Trans. Comput. Aided Des. Integrated Circuits Syst. 22 (1) (2003) 1504–1520.
- [8] P.J. Ashenden, G.D. Peterson, D.A. Teegarden, The System Designer's Guide to VHDL-AMS, 2003.
- [9] G. Sirakoulis, A TCAD system for VLSI implementation of the CVD process using VHDL, VLSI J. Integration 37 (1) (2004) 63–81.
- [10] V. Berouille, R. Khouri, T. Vuong, S. Tedjimi, Behavioral modeling and simulation of antennas: radio-frequency identification case study, Proceedings of the International Workshop on Behavioral Modeling and Simulation, 2003, pp. 102–106.
- [11] B.F. Romanowicz, Methodology for the Modeling and Simulation of Microsystems, Kluwer Academic Publishers, Dordrecht, 1998.
- [12] C.-J. Shi, A. Vachoux, VHDL-AMS design objectives and rationale, Current Issues in Electronic Modeling, vol. 2, Kluwer Academic Publishers, Dordrecht, 1995, pp. 1–30.
- [13] J. Willis, J. Johnson, Language design requirements for VHDL-RF/MW, IEEE MTT-S Int. Microwave Symp. Dig. 3 (2002) 2093–2095.
- [14] S.P. Levitan, J.A. Martinez, T.P. Kurzweg, M. Shomsky, P.J. Marchand, D.M. Chiarulli, System simulation of mixed-signal multi-domain microsystems with piecewise linear models, IEEE

- Trans. Comput. Aided Des. Integrated Circuits Syst. 22 (2) (2003) 139–154.
- [15] T. Mukherjee, G.K. Fedder, D. Ramaswamy, J. White, Emerging simulation approaches for micromachined devices, *IEEE Trans. Comput. Aided Des. Integrated Circuits Syst.* 19 (12) (2000) 1572–1589.
- [16] F. Gaffiot, K.H.K. Vuorinen, F. Mieveville, I. O'Connor, G. Jacquemod, Behavioral modeling for hierarchical simulation of optronic systems, *IEEE Trans. Circuits Syst. II Analog Digital Signal Process.* 46 (10) (1999) 1316–1322.
- [17] F. Pecheux, C. Lallement, A. Vachoux, VHDL-AMS and Verilog-AMS as alternative hardware description languages for efficient modeling of multidiscipline systems, *IEEE Trans. Comput. Aided Des. Integrated Circuits Syst.* 24 (2) (2005) 204–225.
- [18] (<http://bwrc.eecs.berkeley.edu/classes/icbook/spice/>)
- [19] (<http://www.ansys.com>)
- [20] (<http://www.ansoft.com>)
- [21] (<http://www.comsol.com>)
- [22] J. Roychowdhury, Analyzing circuits with widely separated time scales using numerical PDE methods, *IEEE Trans. Circuits Syst.* (5) (2001) 578–594.
- [23] W.R. Zimmerman, Time domain solutions to partial differential equations using SPICE, *IEEE Trans. Edu.* 39 (4) (1996) 563–573.
- [24] J. Roychowdhury, An overview of automated macromodelling techniques for mixed-signal systems, *Proc. IEEE Custom Integrated Circuits Conf.* (2004) 109–116.
- [25] D.A. White, M. Stowell, Full-wave simulation of electromagnetic coupling effects in RF and mixed-signal ICs using a time-domain finite-element method, *IEEE Trans. Microwave Theory Tech.* 52 (5) (2004) 1404–1413.
- [26] M. Schlegel, F. Bennini, J. Mehner, G. Herrmann, D. Muller, W. Dotzel, Analyzing and simulation of MEMS in VHDL-AMS based on reduced-order FE models, *IEEE Sensors J.* 5 (5) (2005) 1019–1026.
- [27] (http://www.cadence.com/products/custom_ic/ams_designer).
- [28] (http://www.mentor.com/products/ic_nanometer_design/simulation/advance_ms).
- [29] (http://www.dolphin.fr/medal/smash/smash_overview.html).
- [30] L. Lemaitre, C. McAndrew, S. Hamm, ADMS-automatic device model synthesizer, *Proc. IEEE Custom Integrated Circuits Conf.* (2002) 27–30.
- [31] B. Hu, C. Wakayama, L. Zhou, C.-J.R. Shi, Developing device models, *IEEE Circuits Devices Mag.* 21 (4) (2005) 6–11.
- [32] A.E. Ruehli, A. Cangellaris, Progress in the methodologies for the electrical modeling of interconnects and electronic packages, *Proc. IEEE* 89 (5) (2001) 740–771.
- [33] A.T. Alastalo, T. Mattila, H. Seppa, Analysis of a MEMS transmission line, *IEEE Trans. Microwave Theory Tech.* 51 (8) (2003) 1977–1981.
- [34] P.V. Nikitin, C.J.-R. Shi, B. Wan, Modeling partial differential equations in VHDL-AMS, *Proc. IEEE Int. Syst.-on-Chip Symp.* (2003) 345–348.
- [35] M.N. Sadiku, L.C. Agba, A simple introduction to the transmission-line modeling, *IEEE Trans. Circuits Syst.* 37 (8) (1990) 991–999.
- [36] W. Gwarek, Analysis of arbitrarily shaped two-dimensional microwave circuits by finite-difference time-domain method, *IEEE Trans. Microwave Theory Tech.* 36 (4) (1988) 738–744.
- [37] G.K. Fedder, Issues in MEMS macromodeling, *Proceedings of the International Conference on Behavioral Modeling and Simulation*, 2003, pp. 64–69.
- [38] F.H. Branin, Transient analysis of lossless transmission lines, *Proc. IEEE* 55 (11) (1967) 2012–2013.
- [39] P.V. Nikitin, E. Normark, C.J.-R. Shi, Distributed electrothermal modeling in VHDL-AMS, *Proceedings of the IEEE International Workshop on Behavioral Modeling and Simulation*, 2003, pp. 128–133.
- [40] X. Huang, H.A. Mantooth, Event-driven electrothermal modeling of mixed-signal circuits, *Proceedings of IEEE/ACM International Workshop on Behavioral Modeling and Simulation*, 2000, pp. 10–15.
- [41] E. Christen, K. Bakalar, A. Dewey, E. Moser, Analog and mixed signal modeling using the VHDL-AMS language, *IEEE Design Automation Conference Tutorial*, 1999.
- [42] E. Colinet, J. Juillard, S. Guessab, R. Kielbasa, Actuation of resonant MEMS using short pulsed forces, *Sensors Actuators A (Phys.)* 1 (15) (2004) 118–125.
- [43] B.D. Jensen, S. Mutlu, S. Miller, K. Kurabayashi, J.J. Allen, Shaped comb fingers for tailored electromechanical restoring force, *J. Microelectromechanical Syst.* 12 (3) (2003) 373–383.
- [44] R.K. Gupta, Electronically probed measurements of MEMS geometries, *J. Microelectromechanical Syst.* 9 (3) (2000) 380–389.
- [45] W.A. Johnson, L.K. Warne, Electrophysics of micromechanical comb actuators, *J. Microelectromechanical Syst.* 4 (1) (1995) 49–59.
- [46] I.-J. Cho, T. Song, S.-H. Baek, E. Yoon, A low-voltage and low-power RF MEMS series and shunt switches actuated by combination of electromagnetic and electrostatic forces, *IEEE Trans. Microwave Theory Tech.* 53 (7) (2005) 2450–2457.
- [47] G.L. Matthaei, Narrow-band fixed-tuned, and tunable bandpass filters with zig-zag hairpin-comb resonators, *IEEE Trans. Microwave Theory Tech.* 51 (4) (2003) 1214–1219.
- [48] K. Wang, C.T.-C. Nguyen, High-order medium frequency micro-mechanical electronic filters, *J. Microelectromechanical Syst.* 8 (4) (1999) 534–556.
- [49] P.V. Nikitin, V. Jandhyala, D. White, N. Champagne, J.R. Jr., C.-J.R. Shi, C. Yang, Y. Wang, G. Ouyang, R. Sharpe, J.R. Sr., Modeling mixed circuit-electromagnetic effects in electronic design flow, *Proc. IEEE Int. Symp. Qual. Electron. Des.* (2004) 244–249.
- [50] A. Odabasioglu, M. Celik, L.T. Pileggi, PRIMA: passive reduced-order interconnect macromodeling algorithm, *IEEE Trans. CAD Integrated Circuits Syst.* 17 (8) (1998) 645–654.
- [51] Y. Liu, L.T. Pileggi, A.J. Strojwas, Ftd: frequency to time domain conversion for reduced-order interconnect simulation, *IEEE Trans. Circuits Syst.* 48 (4) (2001) 500–506.



Pavel V. Nikitin received the B.S. and M.S. degrees in electrical engineering from Utah State University, Logan, UT, in 1994 and 1998, respectively, the B.S. degree in physics from Novosibirsk State University, Novosibirsk, Russia, in 1995, and the Ph.D. degree in electrical and computer engineering from Carnegie-Mellon University, Pittsburgh, PA, in 2002. In Summer 1999, he was a Software Design Engineer with the Ansoft Corporation, Pittsburgh, PA. In Summer 2000, he was a Design Development Engineer with the Microelectronics Division, IBM Corporation, Essex Junction, VT. In 2002, he joined the Department of Electrical Engineering, University of Washington, Seattle, as a Research Associate, where he was involved with computer-aided design of mixed-technology systems-on-chip. In 2004, he joined the Intermec Technologies Corporation, Everett, WA, where he is currently a Lead Engineer with the RFID Intelligat Engineering Department involved with the design and development of antennas for RFID tags. He has authored over 40 technical publications. He also has several patents pending. Dr. Nikitin was the recipient of the ECE Teaching Assistant of the Year Award presented by Carnegie-Mellon University.



C.-J. Richard Shi received the Ph.D. degree in computer science from the University of Waterloo, Waterloo, Ontario, Canada, in 1994. From 1994 to 1998, he worked at Analog (now part of Synopsys), the University of Iowa, and Rockwell Semiconductor Systems (now Conexant Systems). In 1998, he joined the faculty of the University of Washington, Seattle, WA, where he is currently Professor of Electrical Engineering.

His research interests include computer-aided design and test of mixed-signal integrated circuits, as well as VLSI implementation of communication systems. He received several awards for his research, including a Doctoral Prize from the Natural Science and Engineering Research Council of Canada in 1995, a CAREER Award from the National Science Foundation in 2000, a Best Paper Award from the IEEE VLSI Test Symposium in 1998, a Best Paper Award from the IEEE/ACM Design Automation Conference in 1999, and a Best Paper in Session Award from SRC-Tech Conf in 2003. He has supervised 15 PhD students and post-doctoral fellows.

He is a Fellow of IEEE. He is a key contributor to IEEE std 1076.1-1999 (VHDL-AMS) standard for the description and simulation of mixed-signal circuits and mixed-technology systems. He funded IEEE International Behavioral Modeling and Simulation (BMAS) Conference in 1997. He has served as an Associate Editor, as well as a Guest Editor, of the IEEE Transactions on Circuits and Systems—II, Analog and Digital Signal Processing. He is currently serving as an Associate Editor of IEEE Transactions on Computer-Aided Design of Integrated Circuits and Systems and IEEE Transactions on Circuits and Systems-II: Express Briefs.